Magnetostatic spin-wave modes of a ferromagnetic multilayer

P. Grünberg and K. Mika
Institut für Festkörperforschung, Kernforschungsanlage Jülich GmbH, D-5170 Jülich, West Germany
(Received 14 July 1982)

The spin-wave spectrum of a ferromagnetic multilayer is derived in the dipolar-magnetostatic limit. Restrictions are imposed with respect to in-plane magnetization M_s and propagation of the spin waves in plane and perpendicular to M_s. A formula is derived from which the spin-wave branches of a multilayer with a finite number N of magnetic layers can easily be calculated. In the limit of infinitely large N the solutions form a band whose edges and density of states are given by simple expressions. The existence of an additional singular solution depends on the ratio of the thicknesses of magnetic and nonmagnetic layers. We show that these modes can be classified by an integer number j, where $j=1,\ldots,N-1$, and derive a relation between j and the amplitude distribution. As an experimental test of these theoretical results we have also observed the multilayer modes by means of light scattering, and we find good agreement between theory and experiment.

I. INTRODUCTION

Owing to the rapid development in evaporation techniques, there is now a strong interest in modulated structures and multilayer systems. Also, layered structures of alternating magnetic and nonmagnetic films have been investigated.[1,2] Some novel and interesting properties, in particular with respect to the static magnetization, have been reported. Since in many cases the information was mainly drawn from ferromagnetic resonance (FMR) experiments, we have considered it worthwhile to explore the possible spin-wave modes of such a ferromagnetic multilayer and also to attempt for the first time to attack the problem of a multilayer consisting of an infinitely large number of single layers. This work can also be regarded as an extension and continuation of some previous work on ferromagnetic double layers.[3]

The basic physical assumptions as well as the way they are exploited mathematically go back to the work of Damon and Eshbach (DE).[4] For this reason and also in order to have some important symbols and equations conveniently at hand, we find it appropriate to introduce the topic by repeating a few short sections out of the DE article. After linearization, the equation of motion reads in the component form

$$4\pi m_x=\kappa\frac{\partial\Psi}{\partial x}-i\nu\frac{\partial\Psi}{\partial y}\ ,\qquad 4\pi m_y=i\nu\frac{\partial\Psi}{\partial x}+\kappa\frac{\partial\Psi}{\partial y}\ . \tag{1.1}$$

Here m_x and m_y are the transverse precessing moments of the magnetization whose static part points in the z direction. The related h-field components are written in terms of a magnetic potential Ψ:

$$h_x=\frac{\partial\Psi}{\partial x},\quad h_y=\frac{\partial\Psi}{\partial y}\ . \tag{1.2}$$

Physically, this means that Eddy currents are neglected. Here the following abbreviations have been used:

$$\kappa=\frac{\Omega_H}{\Omega_H^2-\Omega^2},\quad \nu=\frac{\Omega}{\Omega_H^2-\Omega^2}\ ,\qquad \Omega_H=\frac{H_0}{4\pi M_s},\quad \Omega=\frac{\omega}{\gamma 4\pi M_s}\ . \tag{1.3}$$

H_0 is the external field, M_s the sample magnetization, and γ the gyromagnetic ratio. In the way it is written here the formalism applies only to a thin ferromagnetic film or plate, strictly extending infinitely in the y and z direction. Only this case will be treated here.

With the use of the equation of motion, the boundary conditions for m and h that follow from Maxwell's equations can be written in terms of the potential Ψ, to yield

$$(1+\kappa)\frac{\partial\Psi^{\text{int}}}{\partial x}-i\nu\frac{\partial\Psi^{\text{int}}}{\partial y}=\frac{\partial\Psi^{\text{ext}}}{\partial x} \tag{1.4}$$

and

$$\Psi^{\text{int}}=\Psi^{\text{ext}}$$

at the interface between magnetic and nonmagnetic matter. Here Ψ^{int} is the potential inside magnetic matter and Ψ^{ext} the same outside.

Following the DE theory, we write the potential Ψ^{int} in the form

$$\Psi^{\text{int}}=X^{\text{int}}e^{iky}\,, \tag{1.5}$$

which means that we restrict ourselves now to propagating waves in the y direction, the related wave vector being k. The DE theory shows that the same k appears also in the x dependence X^{int} of Ψ^{int}, which can be written as

$$X^{\text{int}}=ge^{kx}+he^{-kx}\,. \tag{1.6}$$

The coefficients g and h must still be determined. The potential outside magnetic matter is written down in the same form, but by exploiting the conditions (1.4) at the two surfaces the related coefficients can be eliminated. What remains are the following two equations for g and h:

$$\begin{aligned}&(\kappa+\nu)g+(\nu-\kappa-2)e^{kd}h=0\,,\\&(\kappa+\nu+2)e^{kd}g+(\nu-\kappa)h=0\,.\end{aligned} \tag{1.7}$$

Here d is the thickness of the film or plate, and the other symbols have been defined above. We now introduce a new quantity w, which is defined by

$$w=1+\frac{(\nu-\kappa-2)(\kappa+\nu+2)}{\kappa^2-\nu^2}\,, \tag{1.8}$$

and (1.7) only has solutions if

$$w=1-e^{-2kd}\,. \tag{1.9}$$

This is the DE surface mode. From the definition (1.8) for w one can show that (1.9) is equivalent to

$$\Omega^2=\Omega_H^2+\Omega_H+\tfrac{1}{4}(1-e^{-2kd})\,, \tag{1.10}$$

which is the usual way of writing this solution. Using the quantity w, however, has the great advantage that all magnetic parameters have been normalized out, and the possible range of values obviously is between 0 and 1. So far we have only repeated parts of the DE theory with some slight modifications in the nomenclature. It is straightforward to extend this formalism to the case of more than one film or plate. Here we want to treat the case of an arbitrary number of identical films which are equally spaced such that a periodic structure results. In the limit of infinitely many films, the solutions become particularly simple. We will also briefly discuss possibilities of testing these results experimentally and show that the observation of these modes by means of light scattering establishes the agreement between theory and experiment.

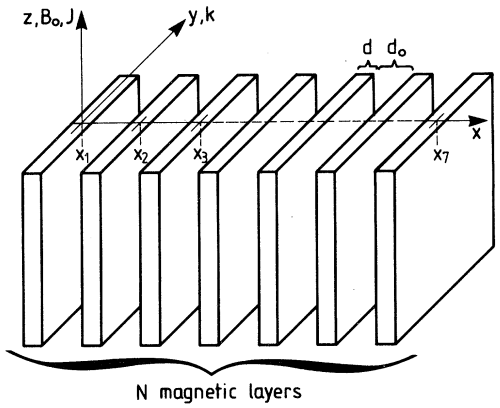

FIG. 1. Ferromagnetic multilayer. There are N (here $N=7$) magnetic layers of thickness d separated by a distance d_0. The layers are supposed to have infinite extent in the $+y,+z$ directions, the external field B_0 and magnetization J ($\triangleq 4\pi M_s$) are oriented along z, and spin-wave propagation k is along y.

II. MODE FREQUENCIES

The case of N magnetic layers of magnetization M_s and thickness d separated by nonmagnetic spacer layers of thickness d_0 that we want to treat here is illustrated in Fig. 1. We introduce a coordinate system in such a way that the midplanes of the films intersect the x axis at points x_l ($l=1,\ldots,N$), and we choose $x_1=0$. Then $x_l=l-1(d_0+d)$. In analogy to (1.6) we write the following for the x dependence of the potential in the lth layer:

$$X_l=g_l\exp[k(x-x_l)]+h_l\exp[-k(x-x_l)]\,. \tag{2.1}$$

Here we have suppressed the index int of Eq. (1.6) because we now refer always to potentials inside magnetic matter. The potentials in the nonmagnetic spacer layers can be written in the same form but with the use of other coefficients. These can be eliminated just in the same way as indicated above for the single layer by using the boundary conditions (1.4). What follows are two relations for the coefficients of adjacent layers:

$$\begin{aligned}&m_1g_l+m_2h_l+m_3g_{l+1}+m_4h_{l+1}=0\,,\\&m_5g_l+m_6h_l+m_7g_{l+1}+m_8h_{l+1}=0\,.\end{aligned} \tag{2.2}$$

Here

$$m_1=(\kappa+\nu+2)\exp(kd),\quad m_2=(\nu-\kappa),\quad m_3=-(\kappa+\nu+2)\exp(-kd_0)\,,$$
$$m_4=-(\nu-\kappa)\exp(kd)\exp(-kd_0),\quad m_5=(\kappa+\nu)\exp(kd),\quad m_6=(\nu-\kappa-2)\,, \tag{2.3}$$
$$m_7=-(\kappa+\nu)\exp(kd_0),\quad m_8=-(\nu-\kappa-2)\exp(kd)\exp(kd_0)\,.$$

There are as many pairs of such equations as there are spacer layers, i.e., $N-1$ pairs for the N-fold multilayer. We complete this set of $2N-2$ equations for the $2N$ coefficients g_l,h_l by adding the two equations

$$m_a g_1+m_b h_1=0,\quad m_\alpha g_N+m_\beta h_N=0\,, \tag{2.4}$$

which, in the same way as (1.7), come from the two outer surfaces on the first and last magnetic layer of the system. From (1.7) we have

$$m_a=(\kappa+\nu),\quad m_b=(\nu-\kappa-2)\exp(kd),\quad m_\alpha=(\kappa+\nu+2)\exp(kd),\quad m_\beta=\nu-\kappa\,. \tag{2.5}$$

This set of $2N$ equations has solutions if the associated determinant vanishes. Hence

$$\begin{vmatrix}
m_a & m_b & & & & & & \\
m_1 & m_2 & m_3 & m_4 & & & & \\
m_5 & m_6 & m_7 & m_8 & & & & \\
 & & m_1 & m_2 & m_3 & m_4 & & \\
 & & m_5 & m_6 & m_7 & m_8 & & \\
 & & & & \ddots & & & \\
 & & & & m_1 & m_2 & m_3 & m_4 \\
 & & & & m_5 & m_6 & m_7 & m_8 \\
 & & & & & & m_\alpha & m_\beta
\end{vmatrix} =0\,, \tag{2.6}$$

where we have indicated only nonzero elements and there are $N-1$ framed 2×4 submatrices.

By applying the usual operations which leave the zeros of a determinant unchanged, Eq. (2.6) can be written in a form involving only a three-band determinant. Since in the first row this contains only one element equal to 1, we can reduce it to a determinant of dimension $2N-1$ and Eq. (2.6) now becomes

$$P_N=\begin{vmatrix}
b & -1 & & & & & & \\
w & -c & -aw & & & & & \\
a & & b & -1 & & & & \\
 & & w & -c & -aw & & & \\
 & & & a & \ddots & & & \\
 & & & & & -aw & & \\
 & & & & a & b & -1 & \\
 & & & & & w & -c & -aw \\
 & & & & & & -a & w-b
\end{vmatrix} =0\,. \tag{2.7}$$

Here the boxes along the main diagonal appear $N-1$ times and we have set

$$a=\exp(-kd_0)\exp(-kd)\ ,$$
$$b=1-\exp(-2kd)\ , \tag{2.8}$$
$$c=1-\exp(-2kd_0)\ ,$$

and used the quantity w defined in (1.8). The parameters a,b,c characterize the system, and we are looking for solutions in w. Suppose w has been found, then from its definition (1.8) and the relations (1.3) the spin-wave frequency ω is given by

$$\omega=\gamma[w(J/2)^2+B_0^2+B_0J]^{1/2}\ . \tag{2.9}$$

B_0 is the external field and J ($\triangleq 4\pi M_s$) the sample magnetization. Note that at this point we go from the cgs over to the SI nomenclature. The cgs system was frequently used in earlier work, including the DE article, but for the comparison with experiment we favor the SI units. Changing the units here is particularly easy because w is dimensionless.

For the limiting values of w we obtain

$$w=0\rightarrow\omega=\gamma\sqrt{B_0(B_0+J)}\ ,$$
$$w=1\rightarrow\omega=\gamma(B_0+J/2)\ . \tag{2.10}$$

The first case corresponds to the dipolar volume mode and the second to a DE surface mode on a half space.[4]

For a finite number of layers, N, one could in principle stop here and treat the problem numerically further. Since we are mainly interested in the limiting case $N\rightarrow\infty$, we simplify the problem in the following way. First, after some algebra, we find the following recurrence relation for the determinants associated with the $N+1$-, N-, and $N-1$-fold layer

$$P_{N+1}+[bc-(1+a^2)w]P_N+a^2w^2P_{N-1}=0\ , \tag{2.11}$$

where

$$P_1=w-b\ ,$$
$$P_2=(w-bc)(w-b)-a^2bw\ . \tag{2.12}$$

$P_1=0$ indeed yields the DE mode of a single layer whereas $P_2=0$ is identical with the quadratic equation which has previously been found for the double layer.[3] Equation (2.11) is a linear recurrence relation for P_N with a coefficient which is quadratic in w. P_N therefore does not fall into the class of the orthogonal polynomials.[5] Since the determinant of Eq. (2.7) can also be written in the form of a special type of fractional chains, Eq. (2.11) and the treatment that now follows can also be applied to evaluate these. These more mathematical aspects are beyond the scope of this paper and are planned to be communicated elsewhere.[6] The solution of Eq. (2.11) follows if we set

$$P_N=\lambda^N\ . \tag{2.13}$$

Insertion of (2.13) into (2.11) yields a quadratic equation in λ which has the two solutions

$$\lambda_{1,2}=\tfrac{1}{2}[(1+a^2)w-bc]\pm\tfrac{1}{2}\{[(1+a^2)w-bc]^2-4a^2w^2\}^{1/2}\ . \tag{2.14}$$

Hence, $P_N=c_1\lambda_1^N+c_2\lambda_2^N$, and the coefficients c_1,c_2 have to be determined from (2.12). This yields

$$P_N=\frac{P_2}{\lambda_1-\lambda_2}(\lambda_1^{N-1}-\lambda_2^{N-1})-\frac{P_1}{\lambda_1-\lambda_2}(\lambda_2\lambda_1^{N-1}-\lambda_1\lambda_2^{N-1})\ . \tag{2.15}$$

In the following we must distinguish between the two cases where λ_1 and λ_2 of Eq. (2.14) are complex or real.

Case 1. λ_1 and λ_2 of Eq. (2.14) are complex if w lies in the interval

$$\frac{bc}{(1+a)^2}<w<\frac{bc}{(1-a)^2}\ . \tag{2.16}$$

In this case, from (2.14) we obtain $\lambda_1=\lambda_2^*$, and to exploit this feature in a convenient form we write

$$\lambda_1=\alpha+i\beta=re^{i\phi}\ ,$$
$$\lambda_2=\alpha-i\beta=re^{-i\phi}\ , \tag{2.17}$$

where

$$\alpha=\tfrac{1}{2}[(1+a^2)w-bc]\ ,$$
$$\beta=(a^2w^2-\alpha^2)^{1/2}\ ,$$
$$r=aw,\quad \phi=\arctan\frac{\beta}{\alpha}\ .$$

With the new variables, we obtain from Eq. (2.15)

$$P_N=\frac{r^{N-2}}{\sin\phi}\{P_2\sin[(N-1)\phi]-rP_1\sin[(N-2)\phi]\}\ , \tag{2.18}$$

where from (2.16) $\pi>\phi>0$.

P_N as a function of ϕ has the following properties:

(i) For large N the zeros are equally spaced on the ϕ axis, and

(ii) the band edges $\phi=\pi$ and $\phi=0$ are as zeros of P_N asymptotically approached for large N.

These properties are plausible from Eq. (2.18) but are planned to be proved in a more strict mathematical way in a forthcoming paper.[6] Hence for large N the zeros of P_N form a band extending from $\phi=\pi$ to $\phi=0$ or $w=bc/(1+a)^2$ to $w=bc/(1-a)^2$, and the density of solutions $dn/d\phi$ is constant over the ϕ axis.

From $dn/d\phi=\text{const}$ follows that dn/dw is proportional to $d\phi/dw$. Then from (2.17) we find

$$\frac{dn}{dw}=\text{const}\times\frac{|bc|}{2\beta w} . \tag{2.19}$$

β becomes zero at the band edges. Hence the density of states given by Eq. (2.19) is finite in the interval (2.16) but diverges at the band edges. This is a very common feature of a density of states.

Case 2. When λ_1 and λ_2 are real, i.e., outside the range given by (2.16), one can show[6] that for large N and $d_0<d$ the largest zero of P_N approaches $w=1$ asymptotically for large N. To illustrate these features we display a numerical example in Fig. 2. The area between the solid lines starting at $d_0=0$, $w=0$ gives the range defined by Eq. (2.16) and hence represents the spin-wave spectrum in the limit of $N\to\infty$. In addition, there is a singular solution at $w=1$ (solid line) equivalent to the DE mode of the half space when $d_0<d$. We also display the density of states for one particular d_0 as indicated. This shows the divergence at the band edges but note that the divergence is stronger at the lower boundary. This comes from the variable w appearing in the denominator of Eq. (2.19).

To get an idea of what can be expected for a real system, i.e., finite N, we display in Fig. 2 results for a 20-fold layer also. To treat this case, P_N has been written in terms of powers of w where the coefficients of that polynomial can easily be found from the recurrence relation (2.11). Then the usual numerical methods for the zeros of a polynomial have been applied. From inspection of Fig. 2 one can see that the $N=20$ case, both for the frequency band as well as for the distribution of the solutions, already indicates the features of the ∞-fold multilayer.

III. MODE CLASSIFICATION AND AMPLITUDE DISTRIBUTION

For a classification of these modes, we rewrite Eq. (2.18) in the form

$$P_N=P\sin[(N-1)\phi+\psi] . \tag{3.1}$$

This is fulfilled if

$$\tan\psi=\frac{rP_1\sin\phi}{P_2-rP_1\cos\phi} ,$$
$$P^2=\left[\frac{r^{N-2}}{\sin\phi}\right]^2(r^2P_1^2+P_2^2-2rP_1P_2\cos\phi) . \tag{3.2}$$

The importance of Eq. (3.1) is only that it gives a means to classify the solutions, because the jth zero ϕ_j of P_N is given by

$$(N-1)\phi_j+\psi_j=j\pi . \tag{3.3}$$

Hence inside the band defined by Eq. (2.16), the solutions can be classified by the number $j=1,\ldots,N-1$ and in addition we have a solution which forms the surface state as $d_0\to 0$.

Equation (3.1) becomes particularly simple for large N when ψ can be neglected, and we obtain

$$\phi_j=\frac{j}{N-1}\pi \tag{3.4}$$

for the zeros of P_N.

With the use of Eq. (3.3), the classification of the modes by means of j is possible for any value of N, and we now want to find a connection between j and the amplitude distribution of the corresponding mode. This means that we must determine the coefficients g_l,h_l of Eq. (2.1). To reduce the computational effort somewhat we treat only the case $H_0=0$, from which according to the definition (1.3) we get $\kappa=0$. The generalization to $H_0\neq 0$ is also easily possible but does not yield any additional physical insight. Setting $\kappa=0$ we obtain from (1.8) $\nu=2/\sqrt{w}$ and the two Eqs. (2.2) can be written as

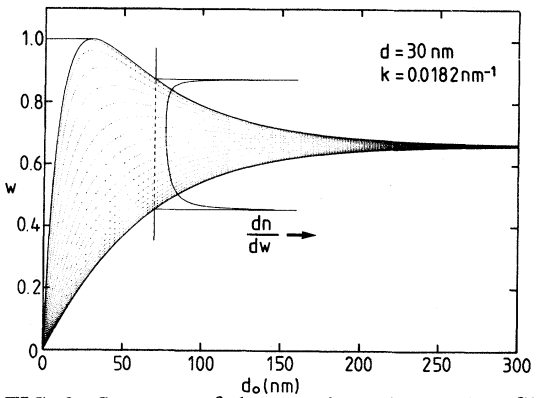

FIG. 2. Spectrum of the quantity w (see text) vs film separation d_0. Solid lines starting at $w=0$ show band edges for $N\to\infty$; solid line starting at $w=1$ represents surface mode for $N\to\infty$. Dotted curves represent $N=20$. Density of states dn/dw vs w for a fixed d_0 (along the broken line) is also displayed.

$$\begin{bmatrix} (1+\sqrt{w})a & \sqrt{1-c} \\ \dfrac{a}{1-c} & \dfrac{1-\sqrt{w}}{\sqrt{1-c}} \end{bmatrix} \begin{bmatrix} g_{l+1} \\ h_{l+1} \end{bmatrix} = \begin{bmatrix} 1+\sqrt{w} & \sqrt{1-b} \\ 1 & \sqrt{1-b}\,(1-\sqrt{w}) \end{bmatrix} \begin{bmatrix} g_l \\ h_l \end{bmatrix}, \tag{3.5}$$

where we have used the parameters a,b,c previously defined. We now introduce the two-component vector

$$v_l = \begin{bmatrix} g_l \\ h_l \end{bmatrix} \tag{3.6}$$

and write Eq. (3.5) in the form

$$v_{l+1} = C v_l \,, \tag{3.7}$$

from which follows

$$v_l = C^{l-1} v_1 \,. \tag{3.8}$$

For the matrix C we obtain from (3.5)

$$C = \begin{bmatrix} \dfrac{w-c}{aw} & \dfrac{c(\sqrt{w}-1)}{w\sqrt{1-c}} \\ \dfrac{c(\sqrt{w}+1)}{w\sqrt{1-c}} & a + \dfrac{ac}{w(1-c)} \end{bmatrix}. \tag{3.9}$$

This matrix and the relation (3.7) is just another way of writing the boundary conditions.

For the determination of the integer powers of C, we need its eigenvalues $\tilde{\lambda}_i$ and eigenvectors e_i,

$$C e_i = \tilde{\lambda}_i e_i \,. \tag{3.10}$$

Let

$$e_1 = \begin{bmatrix} \xi_1 \\ \eta_1 \end{bmatrix}, \quad e_2 = \begin{bmatrix} \xi_2 \\ \eta_2 \end{bmatrix} \tag{3.11}$$

be the eigenvectors. From the eigenvalues we define a matrix

$$D = \begin{bmatrix} \tilde{\lambda}_1 & 0 \\ 0 & \tilde{\lambda}_2 \end{bmatrix}, \tag{3.12}$$

and from the eigenvectors we define

$$S = \begin{bmatrix} \xi_1 & \xi_2 \\ \eta_1 & \eta_2 \end{bmatrix}. \tag{3.13}$$

Then

$$C^l = S D^l S^{-1}$$

and

$$D^l = \begin{bmatrix} \tilde{\lambda}_1^l & 0 \\ 0 & \tilde{\lambda}_2^l \end{bmatrix}. \tag{3.14}$$

The components of S and the two eigenvalues $\tilde{\lambda}_1, \tilde{\lambda}_2$ are found by the usual methods of vector algebra. It turns out that

$$\tilde{\lambda}_{1,2} = \frac{1}{r} \lambda_{1,2} \,, \tag{3.15}$$

where $\lambda_{1,2}$ and r have already previously been determined [Eqs. (2.14) and (2.17)].

For each of the two eigenvectors we are free to choose one component and we set

$$\xi_1 = \xi_2 = -c_{12} \,, \tag{3.16}$$

from which follows that

$$\eta_1 = c_{11} - \tilde{\lambda}_1 \tag{3.17}$$

and

$$\eta_2 = c_{11} - \tilde{\lambda}_2 \,. \tag{3.18}$$

The relation (3.5) establishes only the ratios between the coefficients g_l, h_l, not their absolute values. Experimentally, without external excitation of course, the values corresponding to thermal equilibrium, i.e., the thermal amplitudes would be attained. Here, however, we are free to choose the value of one coefficient and we set

$$g_1 = 1 \,. \tag{3.19}$$

Then from (2.4)

$$h_1 = \sqrt{1-b}\,/(\sqrt{w}-1) \,.$$

The vector v_l describing the lth layer then from (3.8) is given by

$$v_l = C^{l-1} \begin{bmatrix} 1 \\ h_1 \end{bmatrix}. \tag{3.20}$$

By writing C^{l-1} in the form given by Eq. (3.14) and evaluating the resulting relation, one obtains the following, after some algebra:

$$g_l=\frac{-it}{2}(\tilde{\lambda}_1^{l-1}-\tilde{\lambda}_2^{l-1}) + \tfrac{1}{2}(\tilde{\lambda}_1^{l-1}+\tilde{\lambda}_2^{l-1}) ,$$
$$h_l=\frac{-ip}{2}(\tilde{\lambda}_1^{l-1}-\tilde{\lambda}_2^{l-1}) + \frac{h_1}{2}(\tilde{\lambda}_1^{l-1}+\tilde{\lambda}_2^{l-1}) , \tag{3.21}$$

where

$$t=\frac{-1}{2\beta}[bc+(a^2-1)w] , \tag{3.22}$$
$$p=\frac{aw}{\beta(\sqrt{w}-1)\sqrt{1-c}}\left[\frac{c}{2}+\frac{b}{2}\left[c-\frac{c}{w}-1\right]\right] .$$

Using ϕ as introduced by Eq. (2.17), we obtain

$$\tilde{\lambda}_1^{l-1}+\tilde{\lambda}_2^{l-1}=2\cos(l-1)\phi ,$$
$$\tilde{\lambda}_1^{l-1}-\tilde{\lambda}_2^{l-1}=2i\sin(l-1)\phi , \tag{3.23}$$

and hence the coefficients g_l,h_l which describe the potential in the lth layer are given by:

$$g_l=t\sin(l-1)\phi+\cos(l-1)\phi ,$$
$$h_l=p\sin(l-1)\phi+h_1\cos(l-1)\phi . \tag{3.24}$$

The parameters t,p,h_1 are still functions of the spin-wave energy, which is mainly determined by the quantity w. For fixed w and running l, however, Eqs. (3.24) reveal the oscillatory behavior of the potential across the multilayer. This is a typical feature of a standing spin-wave mode. For a large number of films according to Eq. (3.4) we may for the jth solution replace ϕ by

$$\phi_j=\frac{j}{N-1}\pi .$$

Then j just counts the number of oscillations in g_l and h_l from $l=1$ to N. Inside one film, however, the potential remains as is given by Eq. (2.1), i.e., there is exponential decay away from the surfaces which is a typical feature of a surface mode.

Hence the modes which lie inside the band given by Eq. (2.16) have both the features of standing bulk and surface waves. Each of them is described by a set of coefficients g_l,h_l $(l=1,\ldots,N)$, which can be calculated from Eq. (3.24). This is analogous to the usual set of symmetry-adapted linear combinations but not quite the same because one pair g_l,h_l describes only the potential in the lth layer, and there is no superposition of these functions.

IV. EXPERIMENTAL TEST AND CONCLUSIONS

The existence of the DE surface mode has experimentally been established by means of microwaves[7] and by light scattering.[8] In a normal microwave experiment such as in FMR the observed wave vector k is practically zero, in which limit the surface mode merges with the bulk band. This difficulty has been overcome by introducing artificially a finite value of k through the use of stripe couplers.[7] If we set $k=0$ then it follows for the constants defined in (2.8) $a=1$, $b=c=0$. It is easy to show that in this case we get for the multilayer only solutions at $w=0$, corresponding to the bulk mode. Hence an observation of the typical multilayer modes derived here would only be possible by employing stripe couplers just in the same way as for the DE mode.

The other possibility is light scattering. The values of k observed by this method are on the order of 10^5 cm^{-1}. This is a very convenient range of wave vectors because they are just large enough that all features of the DE mode can easily be observed but not too large so the DE mode becomes modified by exchange effects. Apart from single layers the method has already successfully been applied to double layers.[9] In this case in a diagram as displayed in Fig. 2 from the many lower branches

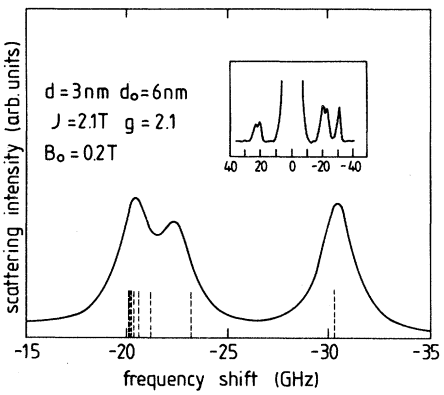

FIG. 3. Light scattering from spin waves in a Fe-Cu multilayer with $N=10$. The main part shows the portion on the Stokes side where scattering is observed. Vertical dashed lines indicate theoretical positions of the modes calculated with the given parameters. The complete spectrum is shown in the inset.

which form a continuum as $N \to \infty$ only one is left over. This was proven experimentally. Still it seems worthwhile to investigate experimentally also the case of more than two layers and to find out if the theoretical predictions hold.

In Fig. 3 we display a representative spectrum from a multilayer composed of ten Fe films with thickness $d = 3$ nm (30 Å) separated by 6 nm thick Cu films. The spectrum shown in the main part of Fig. 3 is a computer plot based on Lorentzian line shapes. Line position, half bandwidth, and oscillator strength are taken from the direct experimental spectrum, which is shown in the inset.

To have a better resolution we display in the main part only the frequency band on the Stokes (S) side where scattering is observed. There is a band at lower and a single line at larger energy shifts. As seen in the inset the band is also observed on the anti-Stokes (aS) side with somewhat reduced intensity, but there is no corresponding line on the aS side for the single peak. This indicates the unidirectional propagation of the corresponding mode.[8] Upon field reversal the spectra on the S and aS side interchange.

As mentioned before, the quantity w which describes the spin-wave spectrum of a multilayer depends on the geometrical relations such as thicknesses and number of films, but is independent of the magnetic parameters. These come in by Eq. (2.9), which relates w with the mode frequency. By variation of the parameters in Eq. (2.9) it is therefore very convenient to fit a given experimental spectrum. The quantity w, which is somewhat more difficult to calculate, can be kept constant during that procedure.

We have calculated the spectrum of w from the geometrical parameters given above. For the magnetic parameters we take the values given in the literature for bulk Fe: J ($\triangleq 4\pi M_s$) $= 2.1$ T and $\gamma = 1.85 \times 10^{11}$ sec^{-1}, which corresponds to a g factor of $g = 2.1$. The theoretical mode spectrum is also shown in Fig. 3 by the dashed vertical lines. We think that the agreement between theory and experiment is quite satisfactory.

The theoretical frequency spectrum of Fig. 3, however, also indicates the limits of the theoretical treatment as presented here. From this it is, for example, not possible to deduce scattering intensities, so it remains unknown how these modes should show up in a light-scattering experiment. An analysis involving the linear response formalism as already performed for single films[10,11] would be necessary for this.

The experimental spectrum of Fig. 3 is only representative, but we have found that altogether in these experiments the peak positions are fairly reproducible. Peak intensities are less reproducible hence both theoretically and experimentally is this point still rather unclear.

These statements indicate along which lines future efforts should go. Another important step in the theory would be the generalization to arbitrary inplane direction of the wave vector. If the thickness of the magnetic films is small enough such a generalization would even yield the full mode spectrum excited at low temperatures. Hence in the usual way of a spin-wave approximation this would allow to calculate the magnetization curve, heat capacity, and various magnetotransport properties of such multilayers. For simplicity and because this case is the easiest one to test experimentally we have confined ourselves to transverse spin-wave propagation, but hopefully the mathematical procedure presented here will turn out to be helpful also in the general case. We have learned recently[12] that Camley, Rahman, and Mills have treated the case $N \to \infty$ for arbitrary in-plane mode propagation. They also present a theoretical study of the light scattering from these modes.

ACKNOWLEDGMENTS

We wish to thank W. Zinn for continued support and interest in this work and U. Funk for assistance in the numerical calculations. Also we acknowledge the skillful technical assistance of R. Schreiber in the experiments.

[1]J. Q. Zheng, C. M. Falco, J. B. Ketterson, and I. K. Schuller, Appl. Phys. Lett. 38, 424 (1981).

[2]Wen-Sheng Zhou, H. K. Wong, J. R. Owers-Bradley, and W. P. Halperin, Physica 108B, 953 (1981).

[3]P. Grünberg, J. Appl. Phys. 51, 4340 (1980); 52, 6824 (1981).

[4]R. W. Damon and J. R. Eshbach, J. Phys. Chem. Solids 19, 308 (1961).

[5]M. Abramowitz and I. Stegun, *Handbook of Mathematical Functions* (Dover, New York, 1965).

[6]K. Mika and P. Grünberg (unpublished).

[7]L. K. Brundle and N. J. Freedman, Elect. Lett. 4, 132 (1968).

[8]P. Grünberg and F. Metawe, Phys. Rev. Lett. 39, 1561

(1977).
[9]P. Grünberg, M. G. Cottam, W. Vach, C. Mayr, and R. E. Camley, Proceedings of the 27th Annual Conference on Magnetism and Magnetic Materials [J. Appl. Phys. 53, 2078 (1982)].
[10]R. E. Camley, T. S. Rahman, and D. L. Mills, Phys. Rev. B 23, 1226 (1981).
[11]M. G. Cottam (unpublished).
[12]R. E. Camley, T. S. Rahman, and D. L. Mills (unpublished).